

DESIGN OF A HIGH-SPEED OSCILLATING BLADE MICROTOME

Ji Wang, Chenglin Li, and Shih-Chi Chen*

Department of Mechanical and Automation Engineering

The Chinese University of Hong Kong

Shatin, N.T., Hong Kong SAR, China

*Email: scchen@mae.cuhk.edu.hk

In this paper, we present the design and characterization of a new high-speed oscillating blade microtome that achieves a substantially higher cutting speed (0 - 300 Hz) and amplitude (0 – 500 μm) than conventional oscillatory tissue cutters; and analytic models that can predict and cutting force, resulting in improved sectioning quality and minimum section thickness. The high cutting amplitude and speed are achieved by driving the cutting mechanism in resonance. Based on the new microtome, we study soft tissue sectioning processes both theoretically and experimentally. The results indicate that a high oscillatory frequency and cutting amplitude will generate higher shear cutting forces, thereby achieving better sectioning results.

DESIGN PRINCIPLE

Previously, we reported a flexure-based vibrating blade microtome [1], integrated with a multiphoton microscope for 3D whole brain imaging. (commercialized by TissueVision Inc.), and an improved design that further minimizes of out-of-plane error motions of the oscillating blade, achieving better performance [2]. In these systems, the operating frequency is designed to be 0 - 100 Hz. The reasons include (1) most commercial systems section soft tissues below 80 Hz; and (2) it is difficult to reduce the out-of-plane motion errors to be $< 1\mu\text{m}$ at high cutting frequency. As our theoretical study has confirmed that a higher cutting frequency yields superior sectioning result [2], in this paper we report the development of a microtome that operates fast enough to exploit the predicted benefit. The design goals include a higher cutting speed (0 - 300 Hz), amplitude (0 – 500 μm), and minimized out-of-plane error motion ($< 500\text{ nm}$).

Figure 1 presents the CAD model of the high-speed oscillating blade microtome. In the design, the oscillatory motion of the blade holder is guided by four parallel beams. The symmetric flexure design ensures a repeatable and linear cutting path as well as high mechanical resonant frequency. A voice coil motor (VCM) directly

drives the blade holder, where the load is applied to the blade holder assembly's center of mass to minimize out-of-plane error motions. During operations, the VCM drives the blade to generate reciprocating linear motions and forces.

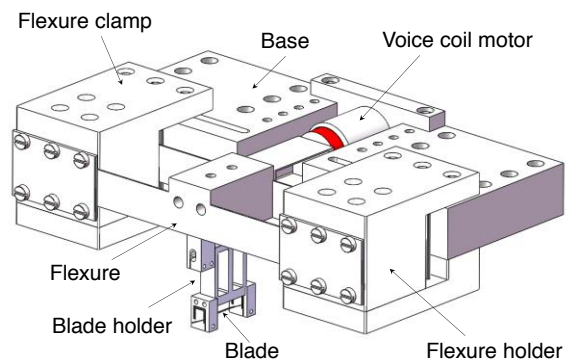


FIGURE 1. CAD model of the high-speed oscillating blade microtome, where a VCM drives the blade holder assembly generating linear cutting paths

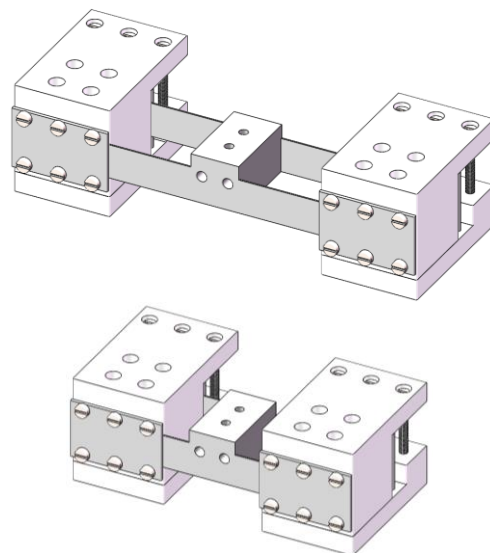


FIGURE 2. Illustration of frequency tuning by adjusting the lengths of clamped beams

As shown in Figure 2, by adjusting the effective lengths of the four parallel beams, the resonant

frequency of the system can be controlled. It is worthwhile to note that the system is purposely operated at a speed close to the resonant frequency to amplify the blade oscillating amplitude. This is required as the VCM has limited force output to generate enough amplitude at high frequency.

Next, we model and study how tuning the resonant frequency can amplify the oscillating amplitude. The driving force generated by the VCM is proportional to the current input before the force reaches the output limit. Assuming the driving force generated by the VCM is $F = F_0 \cos \omega t$, the blade displacement (y) in the oscillating direction can be obtained based on the theory of mechanical vibration [3] as presented in Eq. (1) and (2):

$$y = A \cos(\omega t - \theta) \quad (1)$$

$$A = \frac{1}{\sqrt{(1-s^2)^2 + (2\zeta s)^2}} y_0 \quad (2)$$

where A is the blade vibrating amplitude; $s = \omega/\omega_0$ is the ratio of the driving frequency to the system natural frequency; and y_0 is the blade displacement corresponding to a static loading with the same force amplitude. Assuming the four parallel beams in Fig. 1 have identical dimensions and the length, width and thickness of each beam are l , b , and t respectively, the stiffness of the structure can be found as:

$$k = \frac{4Ebt^3}{l^3} \quad (3)$$

Accordingly, y_0 and the resonant frequency of the structure can be expressed as:

$$y_0 = \frac{F_0 l^3}{4Ebt^3} \quad (4)$$

$$\omega_0 = \sqrt{\frac{4Ebt^3}{ml^3}} \quad (5)$$

where m is the mass of the blade holder structure. Figure 3 presents simulated dynamic responses of the microtome, where the damping ratio is set to 0.1. In the simulation, we study and observe the system response by (1) doubling the input current; and (2) doubling the input current and shortening the beam length from l to $0.8l$. According to Eq. (5) the new resonant frequency becomes $1.25\omega_0$ when the

beam length is shortened, which is confirmed in Fig. 3. One can observe from Fig. 3 that a very high or low driving frequency ω will result in small blade displacements (A). As at high operating frequency, the VCM has small force output, adjusting the beam length, i.e., adjusting the system resonant frequency, can be an effective way to increase blade displacements, as indicated by the blue curve in Fig. 3.

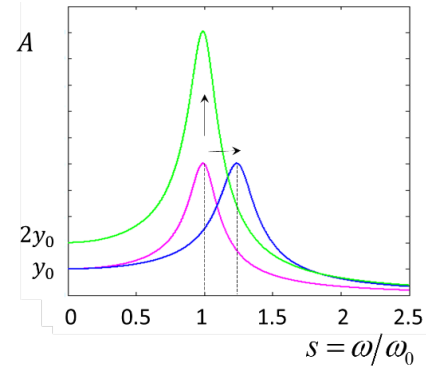


FIGURE 3. Simulated dynamic responses of the frequency tunable oscillating blade microtome

THEORY OF SOFT MATERIAL CUTTING

The general goal of tissue sectioning is to achieve high flatness and thin sections with minimal tissue deformation. In this paper, we model and calculate maximum tissue deformation during the cutting process and use it as an indicator of cutting quality. As reported in our earlier work [2], small cutting forces or small tissue deformation leads to the better the cutting quality.

Previous studies on soft tissue cutting have been focused on understanding how pressing and slicing forces applied to a cutting tool can influence the incision outcome [4-7]. However, these studies and models are limited to static loading conditions and cannot describe dynamic cutting conditions, i.e., cutting tissues with an oscillating blade. In a typical oscillatory tissue cutting process, a blade oscillates transversely at a constant frequency and moves towards a sample at a constant speed (i.e., feed rate), where the entire operation is performed in a water bath to reduce friction and vibration. The operation parameters include (1) blade oscillation frequency (ω), (2) oscillation amplitude (A), and (3) sample feed rate (v). As shown in Fig. 4, we model the oscillatory cutting process by considering a soft sample fixed on a linear stage and moves towards a blade that oscillates transversely. The vibration amplitude

and velocity can be mathematically described as $y = A \cos(\omega t - \theta)$ and $y' = -A\omega \sin(\omega t - \theta)$ respectively. The cutting force applied to the sample from the blade consists of the normal force (F_x) and reciprocating shear force (F_y), where F_y consists of the friction force and adhesion force; note the adhesive force is not considered in the following analysis as it becomes negligible when cutting is performed in the water bath. The sliding motion between the blade and the soft material along the y-direction produces shear forces and can be described as $F_y = \mu F_x$. Previous studies show that the friction coefficient (μ) between a viscoelastic material and a rigid surface is a function of the physical properties of the contact interface as well as the sliding velocity, and the friction coefficient can be modeled as [8]:

$$\mu = \nabla_z \frac{G_2(\omega')}{G^*(\omega')} \quad (6)$$

where ∇_z is the root mean square (RMS) of the gradient of the blade surface, which is a constant in the model; $G_2(\omega')$ and $G^*(\omega')$ are the loss shear modulus and the absolute shear modulus of the material respectively; ω' is the characteristic frequency, defined as $\omega' = 2A\omega/\pi d$, where d is the characteristic diameter of a local contact region between the blade and the material. Note that d is a constant for the same cutting blade [8]. Accordingly, we can express F_y as Eq. (7):

$$F_y = F_y^* \sin(\omega t - \theta) \quad (7)$$

$$F_y^* = \nabla_z \frac{G_2(\omega')}{G^*(\omega')} F_x \quad (8)$$

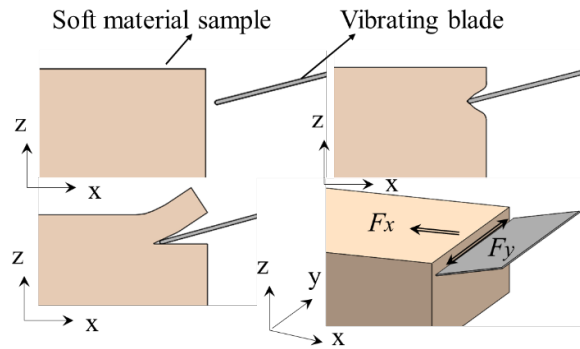


Figure 4 Illustration of the soft material sectioning process and model

The material sectioning process can be divided

into two stages: (1) crack initiation; and (2) crack propagation (Fig. 4). At the first stage, the material in the vicinity of the blade tip deforms under F_x and F_y , where F_x continues to rise as the material is fed to the oscillating blade; and F_y increases with F_x according to Eq. (8). At the second stage, the critical stress condition is reached and a crack is generated and starts to propagate. Note that F_x reaches the maximum value at the critical point and decreases to a stable value as the crack propagates.

At the crack initiation stage, it is assumed that the material around the blade tip is under a line loading of a half space. This assumption is valid because the radius of the blade tip is much smaller than the thickness of the sectioned slice. Based on elastic contact mechanics [9] and assuming Poisson's ratio of the soft material is 0.5, i.e., the material is incompressible, the stress and strain tensor can be obtained in cylindrical coordinates as:

$$\sigma = \begin{bmatrix} -\frac{2F_x \cos \theta}{\pi r L} & 0 & \frac{F_y}{\pi r L} \\ 0 & 0 & 0 \\ \frac{F_y}{\pi r L} & 0 & -\frac{F_x \cos \theta}{\pi r L} \end{bmatrix} \quad (9)$$

$$\epsilon = \begin{bmatrix} -\frac{F_x \cos \theta}{2G^* \pi r L} & 0 & \frac{F_y}{G^* \pi r L} \\ 0 & \frac{F_x \cos \theta}{2G^* \pi r L} & 0 \\ \frac{F_y}{G^* \pi r L} & 0 & 0 \end{bmatrix} \quad (10)$$

As the cutting frequency increases, soft or viscoelastic materials become stiffer and intuitively one may expect superior cutting results. Experiments show critical fracture stress of soft material varies significantly with loading frequency, but the critical maximum principle strain does not change as much. Accordingly, we use the maximum principle strain to determine the onset of crack [10]. Given the radius of the blade tip as r_0 , the maximum principle tensile stress ϵ_t can be obtained from Eq. (9) as $\epsilon_t = F_y^* / 2 G^* \pi r_0 L$, at the material surface when $\theta = \pi/2$. Notice that ϵ_t is not directly related to the compressive force F_x . As F_y^* is determined by F_x , the crack onset state can be written as:

$$F_{x\max} = \frac{2\pi r_0 L \varepsilon_i G^*(\omega)}{\nabla z G_2(\omega')/G^*(\omega')} \quad (11)$$

As mentioned before, the maximum tissue deformation indirectly indicates the cutting quality. From Eq. (10), one may find that the level of material deformation is determined by a coefficient $F_x/2G^*(\omega)\pi L$. Therefore, we define the reciprocal of the deformation coefficient as the factor of sectioning quality, i.e., $K = 2G^*(\omega)\pi L/F_{x\max}$. It can be expressed as Eq. (12). Note that the higher K , the better the sectioning quality.

$$K = \frac{\nabla z G_2(\omega')/G^*(\omega')}{r_0 \varepsilon_0} \quad (12)$$

Since ∇z , r_0 and ε_0 are all constants, K is determined by $G_2(\omega')/G^*(\omega')$ which is determined by the material property and blade speed. Generally, for soft materials, G_2/G^* increases with frequency until it converges to 1. Therefore, we can conclude that a microtome will produce better cutting results at high blade oscillation frequency. The high cutting frequency advantage becomes negligible when G_2 is close to G^* .

CUTTING EXPERIMENTS

To demonstrate and study the advantage of high-speed sectioning, we perform experiments on agarose gel samples (2% and 2.5% concentration) and slice them into sections of 500 μm thick. The entire cutting process is performed in water; and thus the sectioned gel floats on the water surface instead of adhering to the blade. During the experiments, the forces in different directions are measured, i.e., F_x (i.e., sample feeding force) and F_y (blade cutting force); blade vibration frequency (ω) is set to 40 Hz, 100 Hz and 200 Hz; the vibration amplitude is set to 100 μm , 200 μm , and 400 μm ; and the sample feed rate (u) is set to 0.1 mm/s.

Figure 5 presents the experimental results plotted with the theory prediction from Eq. (11), where each data point represents a successful experiment of different sectioning parameters. We find that at low sectioning frequency (40 Hz), the microtome fails to section the agarose gel when $A = 100 \mu\text{m}$. At 200 Hz the microtome successfully sections all gels under all experimental conditions. Note that at 200 Hz the cutting force ($F_{x\max}$) is lower which means tissue deformation is smaller. The mathematical expression of complex shear modulus of

agarose gel is reported in [11].

The experimental and theoretical results proves the advantage of high frequency sectioning that when $\omega = 200$ Hz the lowest cutting force $F_{x\max}$ is produced for each blade vibration amplitude. Notably, Figure 6 also shows that at the same frequency and feed rate, high cutting amplitudes contribute to low cutting force. For example, when $A = 400 \mu\text{m}$, smooth sections can be obtained under all cutting frequencies and feed rates. Although the results suggest that a combination of high cutting frequency and amplitude is preferred, the curves of $F_{x\max}$ tend to converge, which means increasing the parameters only have limited effect. Moreover, driving the blade to operate at high amplitude and frequency simultaneously is mechanically difficult to achieve and can magnify the out-of-plane error motions, leading to inferior cutting results.

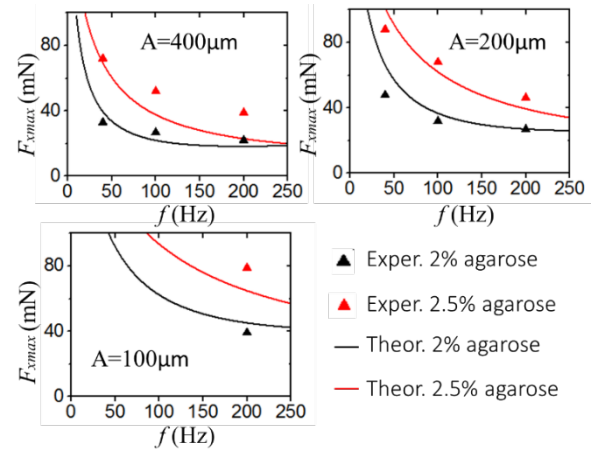


FIGURE 5. The measured and theoretical $F_{x\max}$ for each experiment group

Figure 6 presents our recent results of successive tumor sectioning based on the new microtome, where the tumor is prepared to have a size of $10 \times 10 \times 10 \text{ mm}^3$. Each resulting section is 200 μm in thickness. The sectioning is performed at 200 Hz with a blade amplitude of 200 μm and a sample feed rate of 0.1 mm/s.

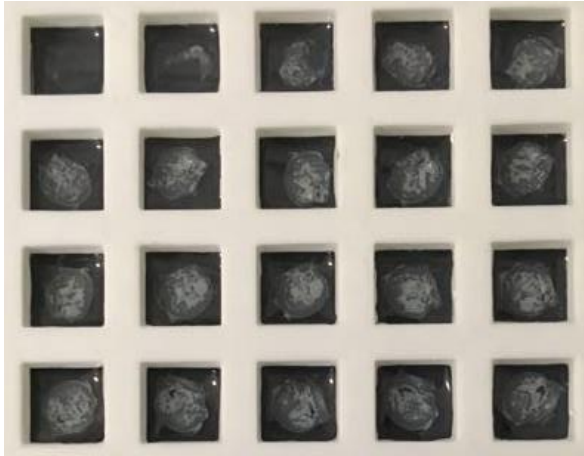


FIGURE 6. *Successive tumor sectioning with a section thickness of 200 μm*

CONCLUSION

In conclusion, we have developed (1) a high-speed oscillating blade microtome that operates in resonance, achieving a tunable operating frequency (0 – 300 Hz) and amplitude (0 – 500 μm); and (2) parametric models that can predict the cutting force and the sectioning quality of any soft samples. Experiments have been performed on agarose gel and tumor samples to verify the model accuracy as well as the capability of the new microtome with a range of different cutting parameters.

ACKNOWLEDGMENT

This work is supported by the HKSAR Research Grants Council (RGC), General Research Fund (GRF), CUHK 14201214.

REFERENCES

- [1] Chen S, Panas R, Culpepper ML, Ragan T. Design of a Precision Flexure-based Vibration Microtome for Whole Organ Imaging. Proc. of the Annual Meeting of the ASPE, San Diego, CA, Oct. 2012, pp.186-89.
- [2] Wang J, Chen S. Study of Soft Tissue Cutting based on a Precision Vibrating Blade Microtome. Proc. of the Annual Meeting of the ASPE, Austin, TX, USA, Nov. 2015, pp. 100-104.
- [3] Bishop RED, Johnson DC. The Mechanics of Vibration. Cambridge University Press. Cambridge. 2011.
- [4] Atkins AG, Xu X, Jeronimidis G. Cutting, by 'Pressing and Slicing,' of Thin Floppy Slices of Materials Illustrated by Experiments on Cheddar Cheese and Salami. Journal of Materials Science. 2004; 39: 2761-2766.
- [5] Reyssat E, Tallinen T, Le Merrer M, Mahadevan L. Slicing Softly with Shear. Phys. Rev. Lett. 2012; 109(24): 244301.
- [6] Han P, Ehmann K. Study of the Effect of Cannula Rotation on Tissue Cutting for Needle Biopsy. Med. Eng. Phys. 2013; 35: 1584.
- [7] Mahvash M, Dupont PE. Mechanics of Dynamic Needle Insertion into a Biological Material. IEEE Transactions on Biomedical Engineering. 2010; 57(4): 934-943.
- [8] Popov VL. Contact Mechanics and Friction. Springer. Berlin. 2010.
- [9] Johnson KL, Contact Mechanics, Cambridge University Press, Cambridge, England, 1987.
- [10] Perez N, Fracture Mechanics, Kluwer Academic Publishers, Boston, USA, 2004.
- [11] Chen Q, Suki B, An K. N. Dynamic Mechanical Properties of Agarose Gels Modeled by a Fractional Derivative Model. Journal of Biomechanical Engineering. 2004, 126, 666-671.